# X-RAY RADIOGRAPHIC OBSERVATION OF DIRECTIONAL SOLIDIFICATION UNDER MICROGRAVITY: XRMON-GF EXPERIMENTS ON MASER12 SOUNDING ROCKET MISSION

G. Reinhart[1, 2], H. Nguyen Thi[1, 2], A.Bogno[1, 2], B. Billia[1, 2], Y. Houltz[3], K. Löth[3], D. Voss[4], A. Verga[4], F. de Pascale[4], R.H. Mathiesen[5], G. Zimmermann[6]

[1]Aix Marseille Univ & [(2)] CNRS, IM2NP UMR 6242
Campus Saint-Jérôme, Case 142, 13397 Marseille Cedex 20, France
[3]Swedish Space Corporation, P.O. Box 4207, SE-171 04 Solna, Sweden
[4]European Space Research & Technology Centre, Keplerlaan 1 Postbus 299, 2200 AG Noordwijk, the Netherlands
[5]Dept. of physics, NTNU, N-7491 Trondheim, Norway
[6]ACCESS e.V, Intzestrasse 5, 52072 Aachen, Germany

Keywords: X-ray radiography, Microgravity, Sounding Rocket, Convection, Fragmentation, Solidification, Aluminium

## Abstract

The European Space Agency (ESA) - Microgravity Application Promotion (MAP) programme entitled XRMON (*In situ* X-Ray MONitoring of advanced metallurgical processes under microgravity and terrestrial conditions) aims to develop and perform *in situ* X-ray radiography observations of metallurgical processes in microgravity and terrestrial environments. The use of X-ray imaging methods makes it possible to study alloy solidification processes with spatio-temporal resolutions at the scales of relevance for microstructure formation.

XRMON has been selected for MASER 12 sounding rocket experiment, scheduled in autumn 2011. Although the microgravity duration is typically six minutes, this short time is sufficient to investigate a solidification experiment with X-ray radiography. This communication will report on the preliminary results obtained with the experimental set-up developed by SSC (Swedish Space Corporation). Presented results dealing with directional solidification of Al-Cu confirm the great interest of performing *in situ* characterization to analyse dynamical phenomena during solidification processes.

## Introduction

Many phenomena involved during solidification are dynamic, such as dendrite fragmentation [1; 2], columnar-to-equiaxed transition [3; 4], and equiaxed growth [5-7]. The study of such phenomena by classical approaches like quenching or decanting is not well adapted. Therefore, *in situ* and real-time X-ray imaging should be retained as the method of choice for investigating the solidification front evolution of metallic alloys grown from the melt [8-10]. In addition, for most real solidification processes involving a liquid phase, natural buoyant convection plays an important role and may interact with the microstructure. An important pending issue is to clarify the role of convection on macrosegregation and on microstructure formation of the solidification process [11; 12]. It has been shown that microgravity (μg) environment is an efficient way to eliminate buoyancy and convection to provide benchmark data for the validation of models and numerical simulations [13-17]. In addition, a comparative study of solidification experiments at 1g and μg can also enlighten the effects of gravity. Therefore, in the frame of the XRMON

project, an experimental set-up has recently been developed to perform directional solidification in microgravity conditions with *in situ* X-ray radiography observation. The first solidification experiment in microgravity using this facility is scheduled during MASER 12 sounding rocket mission, in autumn 2011.

This paper is divided into two parts. The first part will present a brief review of some gravity-induced effects on solidification process, investigated by means of synchrotron X-ray radiography. Experiments were carried out at ESRF (European Synchrotron Radiation Facility) in thin Aluminium-based alloys. In the second part of this paper, we will describe the breadboard tests carried out in Stockholm (Sweden) with a prototype of the XRMON-Gradient Furnace set-up. Preliminary results show the high capabilities of this experimental set-up in terms of thermal behaviour, as well as X-ray observation.

## 1. Influence of convection on solidification process

The synchrotron experiments are carried out at the European Synchrotron Radiation Facility (ESRF), inside a Bridgman furnace [18]. *In situ* and real time observation of the solidification process is possible by the use of synchrotron X-ray radiography. The main surface of the sheet-like sample (40 mm x 6 mm x 0.2 mm) is set perpendicular to the incident monochromatic X-ray beam, with energy in the range 14-18 keV. Absorption is the main source of the image contrast and depends on the atomic number of the elements and the solute content. In all radiographic pictures, the solid aluminum microstructures appear in white and the copper-rich liquid in dark grey after an image processing [19]. The optics is chosen to obtain a good compromise between a large field of view (15 x 6 mm$^2$) and a sufficient resolution (pixel size: 7.46 µm).

Initial Solidification Transient

It is well known that even when solidification is performed under both thermal and solutal stabilizing configuration, convection in the melt can nevertheless be strong due to residual transverse gradient, in particular at low growth rates [16; 20]. Indeed, in real experimental configurations there are generally small departures of the initial interface from planarity, even after a long thermal stabilization phase. As solidification proceeds, the solute is rejected at the solid–liquid interface. Due to gravity, the denser Cu-enriched liquid flows towards depressed regions of the front, which results in solute accumulation in those regions. According to the phase diagram, solute accumulation in depressed regions retards solidification and further deepens the solid–liquid interface modulations. This leads to a large macroscopic deformation of the solidification front (steepling phenomena). In addition, the transverse solute gradient gives rise to a transverse microstructure gradient (clustering phenomena), as already shown by *post-mortem* analysis [16].

Figure 1 shows a sequence of images recorded during the initial transient solidification of Al-4wt% Cu. The temperature of the hot zone of the furnace was lowered at a given cooling rate $R_H$ = 1 K/min, while the temperature of the cold zone of the furnace was maintained constant $R_C = 0$ K/min. The average temperature gradient G is about 35.5 K/cm. In this experiment an initially slightly curved smooth interface is observed (figure 1a), owing to a residual transverse temperature gradient *Gy* of about 1 K/cm [21]. When the cooling of the sample begins the growth rate gradually increases as solidification proceeds, leading to the destabilization of the interface first in the center of the sample. The propagation of the morphological instability towards the two sides of the sample is visible in figure 1, as well as the transverse gradient of microstructure (i.e. clustering phenomena). Concomitantly, macroscopic distortion of the solid–liquid interface becomes larger and larger with time, due to fluid flow in the melt (i.e. steepling phenomena). In figure 1, it can be seen that the liquid phase in the two channels becomes darker as solidification proceeds, which confirms an increase in the liquid solute concentration there.
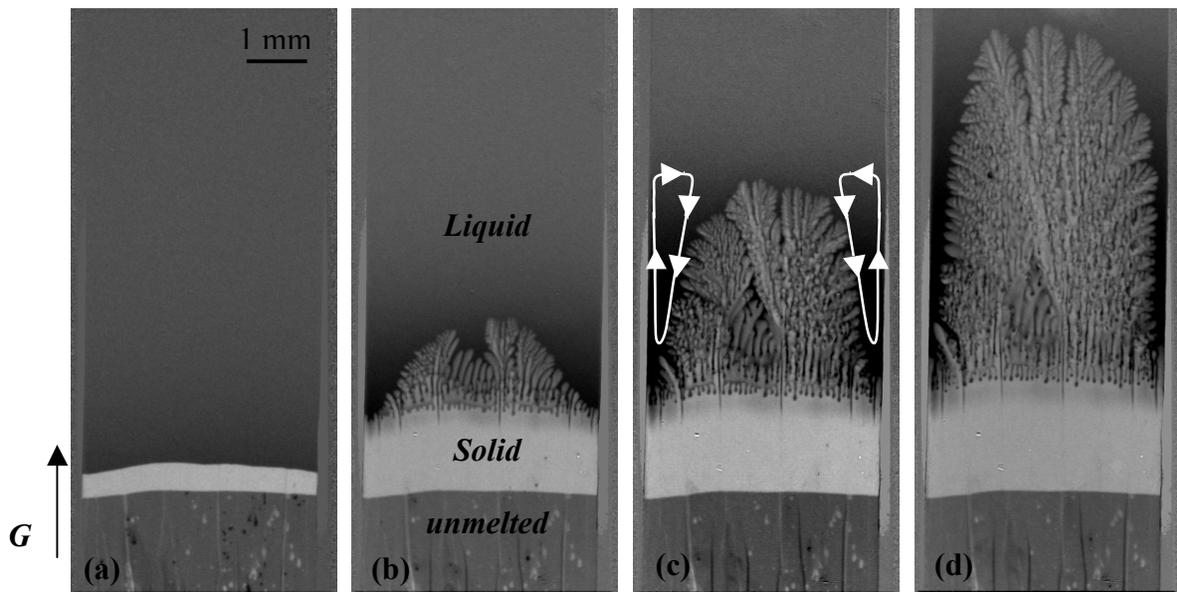
**Figure 1:** Sequence of 4 images showing the progressive deformation of the solid-liquid interface during the initial transient of solidification for Al-4wt% Cu ($R_H$ = 1 K/min; $R_C$ = 0K/min, G=35.5 K/cm). (a) t≈ 20 min; (b) t≈ 40 min; (c) t≈ 50 min; (d) t≈ 60 min

Sedimentation and buoyancy in Al-Cu alloys

Sedimentation or floating of solid parts (i.e. dendrite fragments or equiaxed grains) are two key issues to understand the final microstructure or grain arrangement and can only be analyzed by *in situ* observation [22-25]. In the case of Al-Cu alloys, Ganesan and Poirier [26] calculated the densities of the solid and the liquid phases as function of temperature and composition. They found that below approximately 10 wt% Cu, solid density is larger than liquid density so that we may expect to have solid sedimentation. Above this threshold value, the opposite behavior is anticipated and solid floating assumed. The gravity-settling behavior of equiaxed grains is shown in figure 2, with a sequence of radiographs recorded during an Al − 4 wt% Cu solidification experiment. In this experiment, a few equiaxed grains nucleated above the columnar front (Fig.2a). Some of them remained stuck on crucible wall, but others can fall down due to gravity like the grain indicated by the white circle on the right side of the sample.



**(a) t = $t_0$ + 1320s**        **(b) t = $t_0$ + 1336s**        **(c) t = $t_0$ + 1368s**
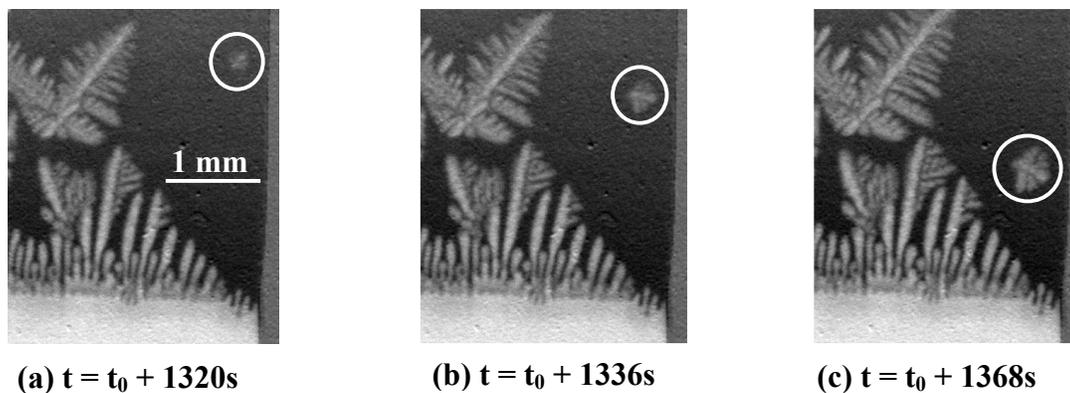
**Figure 2:** Sequence of 3 radiographs showing sedimentation of an equiaxed grain under the effect of gravity during directional solidification of Al-4wt% Cu
($R_H$ = 1.5K/min, $R_C$ = 0, G = 35.5 K/cm) ($t_0$ is the beginning of the cooling).

Live monitoring showed that equiaxed grains grew faster and faster during sedimentation, which is in agreement with the fact that they moved in a richer and colder liquid (Fig.2b and 2c). In addition, they may rotate because of uneven lengthening of their dendrite arms. Finally, the grains stopped to move when they met the columnar front or when their size was comparable to the crucible thickness (Fig.2c). A rough estimate of the sedimentation velocity, typically about 25 μm/s, could be obtained based on successive radiographs. It should be stressed that the falling down of equiaxed grains is enhancing grain packing on the columnar front and may lead to the Columnar – to – Equiaxed Transition when their number and size were large enough [3; 4]. According to this, CET is expected to occur earlier on earth than in microgravity.

The floating behavior of dendrite fragments is shown in figure 3, with a sequence of radiographs recorded during an Al – 10 wt% Cu solidification experiment. In this experiment, fragmentation phenomena of the dendritic columnar microstructure were visible on the left side of the dendritic microstructure (Fig.3a and 3b). The dendrite fragments moved upward because it was buoyant with respect to the surrounding fluid. On contrary to the sedimentation case, the size of the dendrite fragments slightly decreased during their upwards movement because they were gradually melted. A rough estimate of the sedimentation velocities between two successive radiographs gave an approximate value of 60 μm/s. It is worth noticing that these dendrite fragments could not promote Columnar-to-Equiaxed Transition, because they were carried up far into the liquid where they were re-melted. Our conclusions are in agreement with Griffiths et al [27], who analyzed in details the influence of initial solute composition on the formation of equiaxed regions in Al-Cu and Al-Si alloys but during downwards solidification.



(a) t = $t_0$    (b) t = $t_0$ + 44s    (c) t = $t_0$ + 615s    (d) t = $t_0$ + 700s
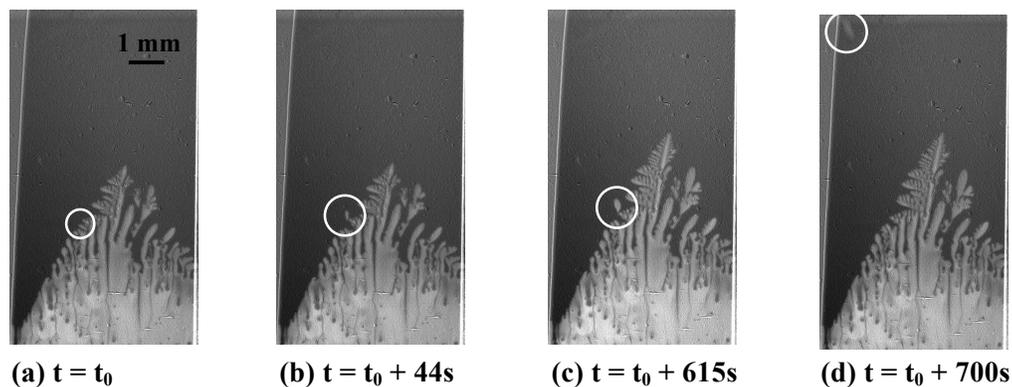
**Figure 3:** Sequence of radiographs showing dendrite fragments moving upwards under the effect of buoyancy during columnar growth of Al-10wt% Cu
($R_H$ = 0.1K/min, $R_C$ = 0.1K/min, G = 23.5 K/cm).

## 2. XRMON – GF project

XRMON-GF device
The conceptual design of the breadboard setup is given in figure 2. It consists of a gradient furnace system for solidification of Al-Cu based alloys and an attached high-resolution X-ray diagnostic system. The metallic samples had a sheet-like geometry with a length of 50mm, a width of 5mm and a roughly constant thickness of less than 0.2mm along the sample. Each sample was mechanically polished down to the desired thickness and then sandwiched between two rectangular glassy carbon plates. To investigate the dynamics of solidification processes, the field of view for the X-ray diagnostics was larger than 5 x 5 mm² with a spatial resolution of

about 5 μm and a temporal resolution of 2-3 Hz. The X-ray source was based on a microfocus transmission target in molybdenum using polychromatic radiation with a peak at 17.5 keV.
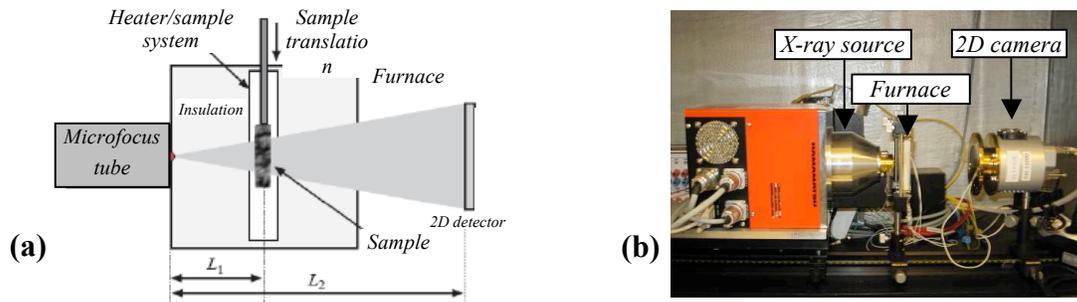


**Figure 4.** (a) Design of the breadboard set-up, (b) picture of the breadboard set-up showing the X-ray source (left), the furnace (very close to the microfocus source) and the detector (right).

Initial transient during directional solidification of Al - 10 wt% Cu alloy

Fig.5 shows a sequence of radiographs recorded during the initial solidification transient of an Al - 10 wt% Cu alloy for a temperature gradient of 43 K/cm and a cooling rate of the hot heater element of 6 K/min. In Fig.5a (t = $t_0$ + 150s, with $t_0$ the reference time, just before the beginning of the solidification) the first disturbances are visible along the whole interface, following the planar front breakdown induced by the Mullins–Sekerka instability [28]. One can already see in Fig.5a that side branches begin to grow on most of the perturbations, which indicates the inception of the formation of dendrites. At this stage, it is possible to determine an average wavelength $\lambda_i$ for the microstructure, $\lambda_i \approx 180$ μm.
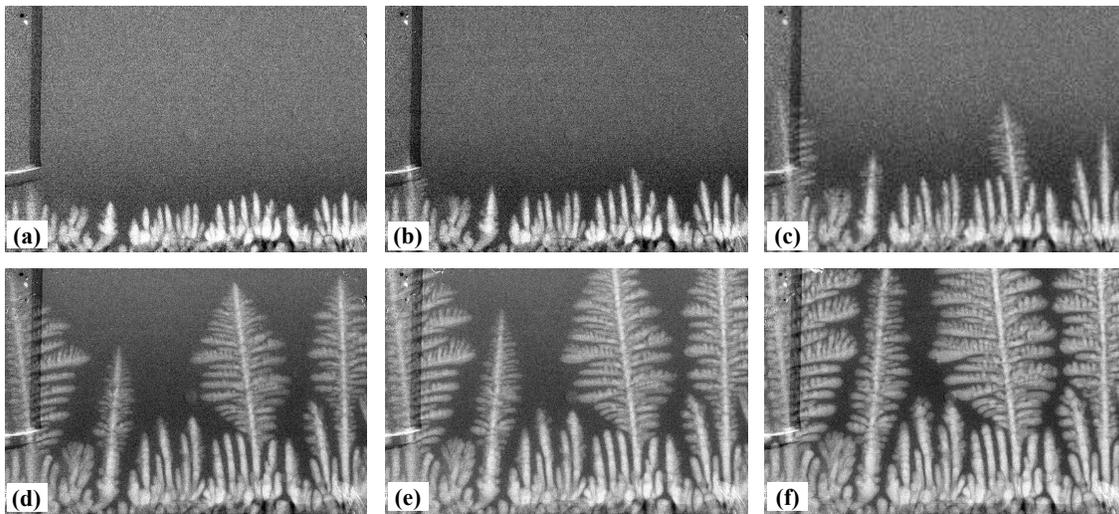


Figure 5. Sequence of radiographs showing the formation of a columnar structure of Al-10wt% Cu (cooling rate = 6 K/min; G ≈ 43 K/cm) (a) t=$t_0$+150s; (b) t=$t_0$+170s; (c) t=$t_0$+200s; (d) t= $t_0$+260s; (e) t=$t_0$+300s; (f) t=$t_0$+400s. $t_0$ is the reference time, just before the beginning of the solidification. Image width=4.5 mm.

Further development of the pattern occurs with a progressive increase of the amplitude of the disturbances (Fig. 5b, t = $t_0$ + 170s), while the liquid ahead of the columnar front becomes darker and darker, due to the solute rejection during the liquid-solid transformation. In the subsequent stages, both the amplitude and lateral size of dendrite increase concomitantly, with solute

84

screening causing a strong decrease of the growth of the neighboring dendrites. The last observed microstructure is mainly composed of several dendrites protruding markedly into the liquid phase with an average final primary spacing $\lambda_f \approx 1\ 260\mu m$ (Fig.5f).

<u>Fragmentation phenomenon during solidification of Al – 20 wt% Cu alloy</u>
One mechanism for the formation of equiaxed grains during the Columnar-to-Equiaxed Transition is the dendrite fragmentation, which is believed to be at the origin of the central equiaxed core region in casting processes [1; 2]. The details of the fragmentation phenomenon are insufficiently understood and controlled. Thus, it is compulsory to confirm the predominance of the fragmentation phenomenon in CET and also to improve the characterisation and understanding of its mechanism, in particular the role of gravity at each step of CET. To achieve this goal, an efficient approach is to perform a comparison between solidification experiments carried out at 1g and in μg, in both cases with *in situ* characterization by means of X-ray radiography. In Fig.6a one can see the gradual establishment of columnar microstructure, as described in the previous section. In this experiment, an equiaxed grain nucleated ahead of the columnar front, on a small heterogeneity. This grain remained fixed and simply continued to grow in interaction with the columnar front. In Fig.6b and Fig.6d, the black circles pinpoint the presence of several dendrite fragments. For Al – 20 wt% Cu, the solid being much lighter than the surrounding liquid, dendrite fragmentation was promoted by buoyancy forces acting on secondary dendrite arms. After the fragmentation, the dendrite pieces were immediately carried away to the upper part of the sample. In this experiment, fragmentation occurred continuously during the growth process. Radiographs made it possible to have a rough estimation of the fragments velocity, about 60μm/s. It is worth noticing that these dendrite fragments could not promote CET, because they were carried up far into the liquid where they were re-melted.
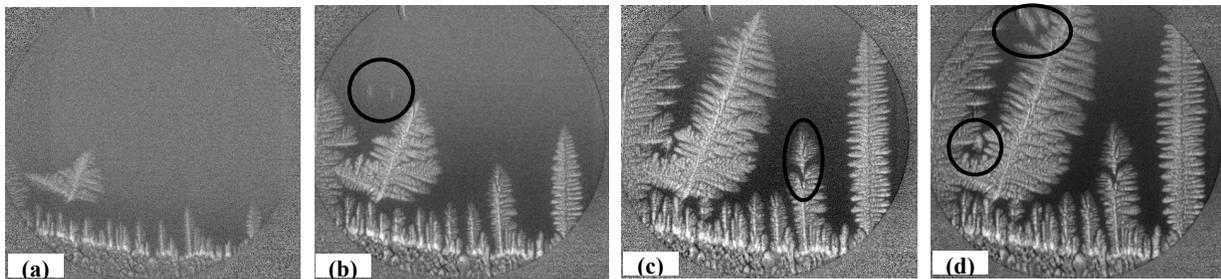


**Figure 6.** Sequence of radiographs during columnar growth of Al – 20 wt% Cu showing several dendrite fragmentations (cooling rate = 20K/min; G = 400 K/cm) (a) t=$t_0$+50s; (b) t=$t_0$+100s; (c) t=$t_0$+150s; (d) t=$t_0$+168s.   $t_0$ is the reference time, just before the beginning of the solidification.

In Fig.6c, the fragmentation of a dendrite primary trunk can also be noticed, indicated by a black ellipse. Its size being close to the sample thickness, the primary trunk fragment could not move far into the liquid phase. This phenomenon was rarely observed compared to the secondary dendrite arm fragmentation, certainly because of the difference in diameter between primary trunk and secondary arms. It has recently been observed by using combined radiography and topography that the rotation of some tenth of degrees around the growth axis of the entire primary trunk during the growth process can occur [29]. This rotation has been interpreted as a consequence of a torque induced by shear stress that builds up with the growth [30]. In our experiments, it was also observed that this phenomenon occurred mainly for a specific crystallographic dendrite direction <110>, which suggests an effect of dendrite morphology.

## Conclusions

This paper reports on a selection of results obtained during metallic alloy solidification experiments characterized *in situ* and in real time by X-ray radiography. Experiments were carried out with both a synchrotron source and a microfocus tube, with a dedicated novel experimental set-up developed in the frame of the ESA-MAP XRMON. These results emphasize the great impact of gravity and convection on the dynamics of the solidification front by showing the influence of convection on the initial solidification transient, the sedimentation/buoyancy of equiaxed grains or dendrite fragments. The next step of the project is to perform an experiment in microgravity environment to obtain purely diffusive transport conditions and then to provide benchmark data for the validation of models and numerical simulations. In addition, a comparative study of solidification experiments at 1g and μg will also enlighten the effects of gravity. This is the goal of the solidification experiment scheduled during MASER 12 sounding rocket mission, in autumn 2011.

## References

1.	H. Jung et al. "Fragmentation in an Al-7 wt-%Si alloy studied in real time by X-ray synchrotron techniques", *International Journal of Cast Metals Research*, *22*(1-4).(2009). 208-211.
2.	D. Ruvalcaba et al. (2007). Fragmentation due to the interaction of solute flow with the dendritic network during the solidification of aluminum alloys. In: *5th Decennial Conference on Solidification processing* (pp. 321-325). Sheffield, U.K.: University of Shefffield, U.K.
3.	H. Nguyen Thi et al. "In-Situ and Real-Time Investigation of Columnar to Equiaxed Transition in Metallic Alloy", *Metall. Mater. Trans. A*, *38-7*.(2007). 1458-1464.
4.	G. Reinhart et al. "in-situ observation of transition from columnar to equiaxed growth in al-3.5 wt% ni alloys by synchrotron radiography", *Modeling of Casting, Welding and Advanced Solidification Processes*, *XI*.(2006). 359-366.
5.	A. Bogno et al. "Application of synchrotron X-ray radiography to the study of dendritic equiaxed microstructure formation in Al-Cu alloys", *Nuclear Instruments and Methods in Physics Research Section B: Beam Interactions with Materials and Atoms*, *268*(3-4).(2010). 394-398.
6.	A. Bogno et al. "In situ analysis of dendritic equiaxed microstructure formation in Al-Cu alloys by synchrotron X-ray radiography", *Transactions of the Indian Institute of Metals*, *62*(4-5).(2009). 427-431.
7.	A. Badillo, & C. Beckermann (2007). Growth of equiaxed dendritic crystals settling in an undercooled melt. In: *5th Decennial International Conference on Solidification processing* (p. 316). Sheffield, UK: University of Sheffield, UK.
8.	R. H. Mathiesen et al. "Time-resolved X-Ray Imaging of Dendritic Growth in Binary Alloys", *Phys. Rev. Lett.*, *83*.(1999). 5062-5065.
9.	H. Yasuda et al. "Direct Observation of stray crystal formation in unidirectional solidification of Sn-Bi alloy by X-ray imaging", *Journal of Crystal Growth*, *262*.(2004). 645-652.
10.	T. Schenk et al. "Application of synchrotron X-ray imaging to the study of directional solidification of aluminium-based alloys", *Journal of Crystal Growth*, *275*.(2005). 201-208.
11.	S. H. Davis "Hydrodynamics Interactions in Directional Solidification", *J. Fluid Mech.*, *212*.(1990). 241-262.

12.    D. T. J. Hurle (1992). *Interactive Dynamics of Convection and Solidification*. Pays-Bas: Kluwer Academic.

13.    C. Giummarra et al. "Sidebranch characteristics of pivalic acid dendrites grown under convection-free and diffuso-convective conditions", *Journal of Crystal Growth*, *274*(1-2).(2005). 317-330.

14.    J. C. LaCombe et al. "Nonconstant tip velocity in microgravity dendritic growth", *Physical Review Letters*, *83*(15).(1999). 2997-3000.

15.    M. B. Koss et al. "Dendritic growth tip velocities and radii of curvature in microgravity", *Metallurgical and Materials Transactions a-Physical Metallurgy and Materials Science*, *30*(12).(1999). 3177-3190.

16.    H. Nguyen Thi et al. "Directional Solidification of Al-1.5wt% Ni alloys under diffusion transport in space and fluid flow localisation on Earth", *J. of Crystal Growth*, *281*.(2005). 654-668.

17.    B. Drevet et al. "Solidification of Aluminum-Lithium Alloys near the Cell/Dendrite Transition - Influence of Solutal Convection", *J. Crystal Growth*, *218*.(2000). 419-433.

18.    A. Buffet et al. "Real-time and in situ solidification of Al-based alloys investigated by synchrotron radiation: a unique experimental set-up combining radiography and topography techniques", *Phys. Stat. Sol.*, *204*(8).(2008). 2721-2728.

19.    A. Buffet et al. "Measurement of solute profiles by means of synchrotron X-ray radiography during directional solidification of Al - 4 wt% Cu alloys", *Materials Science Forum*, *649*.(2010). 331-336.

20.    M. H. Burden et al. "Macroscopic Stability of a planar, cellular or dendritic interface during directional freezing", *J. Cryst. Growth*, *20*.(1973). 121-124.

21.    A. Bogno et al. "Analysis by synchrotron X-ray radiography of convection effects on the dynamic evolution of the solid-liquid interface and on solute distribution during the initial transient of solidification", *Acta Materialia*, *59*(11).(2011). 4356-4365.

22.    B. Appolaire et al. "Free growth of equiaxed crystals settling in undercooled NH4Cl-H2O melts", *Acta Materialia*, *46*(16).(1998). 5851-5862.

23.    A. Ramani, & C. Beckermann "Dendrite tip growth velocities of settling NH4Cl equiaxed crystals", *Scripta Materialia*, *36*(6).(1997). 633-638.

24.    A. Badillo et al. "Growth of equiaxed dendritic crystals settling in an undercooled melt, Part 2: Internal solid fraction", *Journal of Crystal Growth*, *309*(2).(2007). 216-224.

25.    N. Mangelinck-Noël et al. "In situ analysis of equiaxed growth of aluminium-nickel alloys by x-ray radiography at ESRF", *J. Phys. D: Appl. Phys.*, *38*.(2005). 28-32.

26.    S. Ganesan, & D. R. Poirier "Densities of Aluminum-Rich Aluminum-Copper Alloys during Solidification", *Metalurgical Transaction A*, *18A*.(1987). 721-723.

27.    W. D. Griffiths et al. "The influence of bulk liquid natural convection on the formation of the equiaxed regions in Al   Cu and Al   Si alloys", *Materials Science and Engineering: A*, *205*(1-2).(1996). 31-39.

28.    W. W. Mullins, & R. F. Sekerka "Stability of a planar interface during solidification of a dilute binary alloy", *J. Appl. Phys.*, *35*.(1964). 444.

29.    G. Reinhart et al. "In-Situ and real-time analysis of the formation of strains and microstructure defects during solidification of Al-3.5 wt pct Ni alloys", *Metallurgical and Materials Transactions a-Physical Metallurgy and Materials Science*, *39A*(4).(2008). 865-874.

30.    B. Billia et al. "Cumulative moments and microstructure deformation induced by growth shape in columnar solidification", *Phys. Rev Lett.*, *93*(12).(2004). 126105.